

Strong cation ordering in olivine-related (Ni,Fe)-sarcopsides: a combined Mössbauer, X-ray and neutron diffraction study

TORE ERICSSON

*Department of Mineralogy and Petrology
Institute of Geology, University of Uppsala
Box 555, S-75122 Uppsala, Sweden*

AND ANDERS G. NORD

*Section of Mineralogy, Swedish Museum of Natural History
Box 50007, S-10405 Stockholm, Sweden*

Abstract

Olivine-related $(\text{Ni}_{1-x}\text{Fe}_x)_3(\text{PO}_4)_2$ solid solutions with the sarcopside structure have been prepared and equilibrated at 1 bar, 1070 K ($0 \leq x \leq 0.70$). Pure $\text{Fe}_3(\text{PO}_4)_2$ -sarcopside has been prepared hydrothermally. Accurate unit cell dimensions ($P2_1/a$) are given. The cation distribution among the octahedrally coordinated M1 and M2 sites has been determined from Mössbauer spectroscopy between 10 K and 853 K, showing that Ni^{2+} concentrated at the M1 sites with $K_D(\text{Ni,Fe}) \approx 100$. A profile-refinement of $\text{NiFe}_2(\text{PO}_4)_2$ with neutron diffraction data has been done. The average metal–oxygen distances also indicate that nickel preferentially occupies the M1 site. Mössbauer spectra, recorded at low temperatures, show magnetic order. The transition temperature for pure $\text{Fe}_3(\text{PO}_4)_2$ -sarcopside is 44 K. However, the M1 iron does not take part in the magnetic coupling in the temperature region investigated.

Introduction

Four years ago we started a project on cation distributions in solid solutions of synthetic orthophosphates with the farringtonite or graffonite structure (e.g., Annersten et al., 1980; Nord and Ericsson, 1982a,b). We have now continued our work with studies of orthophosphates with the sarcopside structure, which is of additional interest because of its close structural relationship with olivine.

The crystal structure of sarcopside, $(\text{Fe,Mn,Mg})_3(\text{PO}_4)_2$, was determined by Moore (1972). Similar to olivine, sarcopside contains two distinct MO_6 octahedra; these are ordered in edge-sharing trimers, while they are connected in serrated chains in olivine. The cation sites are conventionally denoted M1 and M2. The MO_6 octahedra in sarcopside are similar in size and shape to the corresponding octahedra in olivine. Calvo and Faggiani (1975) have shown that pure nickel orthophosphate is isomorphous with sarcopside. The present paper reports on studies of some $(\text{Ni}_{1-x}\text{Fe}_x)_3(\text{PO}_4)_2$ solid solutions with the sarcopside structure.

Experimental

Batch samples of $\text{Ni}_3(\text{PO}_4)_2$ and $\text{Fe}_3(\text{PO}_4)_2$ were prepared as described by Nord and Kierkegaard (1980) and used in all

preparation procedures. The (Ni,Fe)-sarcopsides were made by heating mixtures of the two pure orthophosphates in evacuated and sealed silica tubes at 1070 ± 10 K for one month and then quenching them in water. Pure $\text{Fe}_3(\text{PO}_4)_2$ -sarcopside and $(\text{Fe}_{0.85}\text{Ni}_{0.15})_3(\text{PO}_4)_2$ were prepared in a hydrothermal Nimonic-105 autoclave at 800 bar, 570 K (7 days).

X-ray powder diffraction data of each sample were obtained at room temperature (295 K) with a Guinier-Hägg type focusing camera ($\text{CrK}\alpha_1$ radiation, KCl internal standard). Neutron powder diffraction data were collected at 295 K at the Studsvik R2 reactor (Studsvik, Nyköping, Sweden) from 3 cm^3 ($\sim 10 \text{ g}$) of powdered $\text{NiFe}_2(\text{PO}_4)_2$ ($2^\circ \leq \theta \leq 43^\circ$, $\Delta\theta = 0.04^\circ$). The average flux was $10^{10} \text{ neutrons} \cdot \text{m}^{-2} \cdot \text{s}^{-1}$ for $\lambda \approx 1.55 \text{ \AA}$.

The Mössbauer spectroscopic investigations were performed with a conventional apparatus working in constant acceleration mode and using transmission geometry. The velocity scale was calibrated using iron foil ($\alpha\text{-Fe}$) recorded at room temperature; centroid shifts (CS) are given relative to $\alpha\text{-Fe}$ at room temperature. The single line source was ^{57}Co in a rhodium matrix ($\sim 20 \text{ mCi}$). The absorbers, containing $\sim 5 \text{ mg}$ of natural iron per cm^2 , were made from the material thoroughly mixed with a plastic transoptic powder ($\sim 100 \text{ mg/cm}^2$), heated at 380 K and then pressed to a thin disc. For measurements at elevated temperatures, the samples were spread on a thin beryllium disc and heated in a vacuum furnace. At temperatures below 77 K, the plastic discs were cooled in a helium flow cryostat ($T \geq 4.2 \text{ K}$). In the subsequent computer fitting procedures, Lorentzian functions were used.

Strategy of the cation distribution study

Preliminary experiments showed that the solubility of $\text{Fe}_3(\text{PO}_4)_2$ in $\text{Ni}_3(\text{PO}_4)_2$ is large, around 70 mole% at 1 bar, 1070 K. Accurate unit cell dimensions showed that the (Ni,Fe)-sarcopsides obey Vegard's law. The observed maximum solubility suggested a strong ordering with Fe^{2+} at the more numerous M2 sites (2/3 of all available cation sites). However, only one ^{57}Fe Mössbauer doublet was resolved in the spectra of both the (Ni,Fe)-sarcopsides and pure Fe-sarcopside at temperatures between 77 K and 853 K. This indicated pronounced overlap of the two Mössbauer doublets. The ordering was finally determined from neutron powder diffraction and magnetic hyperfine Mössbauer spectra.

Results

X-ray diffraction data

$\text{Ni}_3(\text{PO}_4)_2$ (Calvo and Faggiani, 1975) and the (Ni,Fe)-sarcopsides studied here have the space group $P2_1/a$, originally determined for sarcopside (Moore, 1972). Accurate unit cell parameters (Table 1) were obtained by conventional least-squares refinements of Guinier-Hägg data. Unit cell volumes for the $(\text{Ni}_{1-x}\text{Fe}_x)_3(\text{PO}_4)_2$ solid solutions are shown vs. composition in Figure 1; Vegard's law is obeyed within the single-phase region. The solubility of $\text{Fe}_3(\text{PO}_4)_2$ in $\text{Ni}_3(\text{PO}_4)_2$ (at 1 bar, 1070 K) is about 70 mole%, i.e., $0 \leq x \leq 0.70$. For $0.70 \leq x \leq 0.90$, there is a two-phase region (sarcopside + graffonite), whereas for $0.90 \leq x \leq 1$ (still at 1 bar, 1070 K), there is single-phase (Ni,Fe)-graffonite.

At 1 bar, $\text{Fe}_3(\text{PO}_4)_2$ has the graffonite structure with 6,5,5-coordinated cations and with $V = 601.4(4)\text{\AA}^3$ for $Z = 4$ (Kostiner and Rea, 1974), i.e., $V/Z = 150.4(1)\text{\AA}^3$. Hydrothermally prepared $\text{Fe}_3(\text{PO}_4)_2$ -sarcopside has $V = 301.3(2)\text{\AA}^3$ for $Z = 2$ (Table 1), i.e., $V/Z = 150.6(1)\text{\AA}^3$. It is peculiar that the two values for V/Z are almost identical. The cell volumes for $\text{Fe}_3(\text{PO}_4)_2$ - and $(\text{Fe}_{0.85}\text{Ni}_{0.15})_3(\text{PO}_4)_2$ -sarcopsides have been inserted in Figure 1. Note that the extrapolated $V = f(x)$ line for the (Ni,Fe)-sarcopsides passes through these points ($x = 1$ and $x = 0.85$).

Table 1. Unit cell dimensions ($P2_1/a$) at 295 K for the $(\text{Ni}_{1-x}\text{Fe}_x)_3(\text{PO}_4)_2$ sarcopside-type solid solutions

x	a (Å)	b (Å)	c (Å)	β (°)	V (Å ³)
0	10.104(2)	4.698(1)	5.830(1)	91.13(2)	276.7(2)
0.10	10.145(2)	4.700(1)	5.858(1)	91.06(2)	279.3(1)
0.20	10.186(2)	4.703(2)	5.882(1)	91.02(3)	281.7(2)
0.30	10.220(2)	4.707(1)	5.908(1)	91.00(1)	284.2(1)
0.40	10.267(2)	4.712(1)	5.933(1)	90.97(2)	287.0(1)
0.50	10.306(3)	4.717(1)	5.959(2)	90.92(2)	289.6(2)
0.60	10.350(2)	4.724(2)	5.984(2)	90.89(3)	292.5(3)
0.67	10.363(3)	4.732(1)	5.990(1)	90.91(2)	293.7(2)
0.70	10.368(3)	4.735(2)	5.994(1)	90.92(2)	294.2(3)
0.85*	10.419(2)	4.757(1)	6.015(1)	90.94(2)	298.1(2)
1*	10.442(3)	4.787(1)	6.029(1)	90.97(2)	301.3(2)

* These data refer to the hydrothermally prepared phases. The estimated standard deviations are given in parentheses.

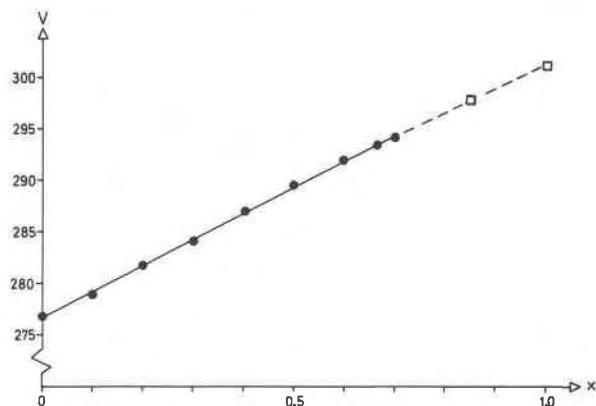


Fig. 1. Unit cell volume V versus composition x for the $(\text{Ni}_{1-x}\text{Fe}_x)_3(\text{PO}_4)_2$ -sarcopsides. The values for $x = 0.85$ and $x = 1$ (□) refer to hydrothermally prepared phases.

Neutron diffraction study of $\text{NiFe}_2(\text{PO}_4)_2$

A neutron diffraction study of $\text{NiFe}_2(\text{PO}_4)_2$ was undertaken to verify the sarcopside structure and with the hope that the interatomic metal-oxygen distances might indicate the cation partitioning. The neutron scattering amplitudes are: $b(\text{Ni}) = 1.03$, $b(\text{Fe}) = 0.95$, $b(\text{P}) = 0.51$, and $b(\text{O}) = 0.575$ (all in 10^{-12} cm units). Data for $2 \leq \theta \leq 43^\circ$ were used, including 200 independent reflections ($\lambda \approx 1.55\text{\AA}$). Due to the unfavorable value of the monoclinic angle of $\text{NiFe}_2(\text{PO}_4)_2$ ($\beta = 90.91^\circ$), there was considerable overlap among the reflections. It was also difficult to estimate the background level. The net intensities were processed by means of the full-profile refinement technique of Rietveld (1969). The parameters refined were: one overall scale factor, three parameters to describe the Gaussian shape of the peaks, four unit cell parameters (to define the mean wavelength), 18 atomic positional parameters and three isotropic temperature factors (for metals, phosphorus and oxygens). Probably due to the overlap among the reflections, it was not possible to refine all parameters at the same time; an iterative procedure had to be used. In the final refinement all positional parameters (but not other) were refined simultaneously. The R_1 value very slowly converged to 0.064 ($R_p = 0.08$, $R_{wp} = 0.09$). The observed and calculated neutron diffraction pattern is shown in Figure 2. The atomic parameters are listed in Table 2. A table of the observed and calculated integrated intensities from the final refinement is available.¹

Some selected interatomic distances in $\text{NiFe}_2(\text{PO}_4)_2$ are given in Table 3. In Pure $\text{Ni}_3(\text{PO}_4)_2$ the average metal-oxygen distances for M1 and M2 are 2.081 and 2.084 Å (Calvo and Faggiani, 1975). In $\text{NiFe}_2(\text{PO}_4)_2$ the corre-

¹ To obtain a copy of these tables, order Document AM-84-245 from the Business Office, Mineralogical Society of America, 2000 Florida Avenue, N. W. Washington, D. C. 20009. Please remit \$5.00 in advance for the microfiche.

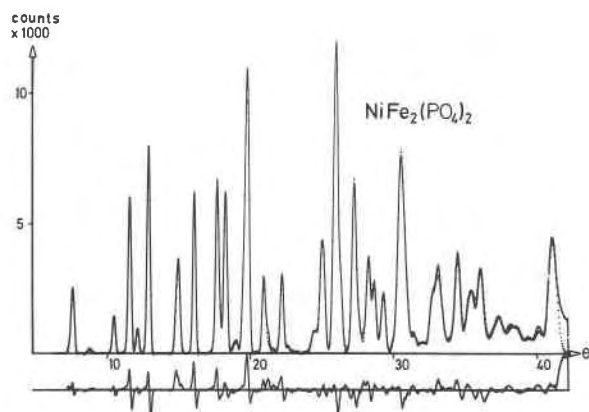


Fig. 2. The least-squares fit obtained between the observed intensities (continuous curve) and calculated intensities (points) from the final full-profile neutron-data refinement of $\text{NiFe}_2(\text{PO}_4)_2$. The discrepancy in the fit, $I_{\text{obs}} - I_{\text{calc}}$, is plotted below on the same scale.

sponding values are 2.11 and 2.15 Å, indicating that the larger Fe^{2+} ions concentrate at the M2 sites. Although the iterative refinement technique used may give overly optimistic standard deviations, these results support the reasonable assumption based on observed conditions in (Ni,Fe)-olivines (Annersten et al., 1982) and the solubility of $\text{Fe}_3(\text{PO}_4)_2$ in $\text{Ni}_3(\text{PO}_4)_2$. A thorough discussion on the standard deviations in Rietveld refinements has been published by Scott (1983). The average P–O bond distance is 1.54 Å, in good agreement with the grand mean value (1.537 Å) calculated for divalent-metal orthophosphates by Nord and Kierkegaard (1980).

Room-temperature Mössbauer data

All spectra were fairly similar in shape (Table 4 and Fig. 3); they had a symmetric intense quadrupole doublet with $\text{CS}/\Delta E_Q \approx 1.2/3.05$ mm/s. Most spectra also had weak traces of a narrow doublet with $\text{CS}/\Delta E_Q \approx 1.3/2.3$ mm/s, originating from negligible amounts of an unidentified impurity. In the fitting procedure, the two peaks in the major quadrupole doublet from the sarcopside were constrained to have equal intensities and half widths W . The widths obtained, 0.24–0.28 mm/s, are characteristic

Table 2. Final atomic parameters obtained from the neutron diffraction study of $\text{NiFe}_2(\text{PO}_4)_2$

Atom	x	y	z	B (Å^2)
M1	0	0	1/2	0.2(1)
M2	0.282(1)	-0.023(1)	0.237(1)	0.2(1)
P	0.093(1)	0.414(2)	0.266(2)	0.5(3)
0(1)	0.107(1)	0.746(2)	0.276(2)	0.1(1)
0(2)	0.460(1)	0.188(2)	0.253(2)	0.1(1)
0(3)	0.179(1)	0.313(3)	0.064(2)	0.1(1)
0(4)	0.158(1)	0.276(2)	0.468(2)	0.1(1)

The estimated standard deviations are given in parentheses.

Table 3. Some interatomic distances (Å) in $\text{NiFe}_2(\text{PO}_4)_2$

M - 0(1)	(x2)	2.12(1)	M2 - 0(1)	2.13(2)	P - 0(1)	1.57(2)
- 0(2)	(x2)	2.12(1)	- 0(2)	2.10(2)	- 0(2)	1.47(2)
- 0(4)	(x2)	2.10(1)	- 0(3)	2.17(2)	- 0(3)	1.58(2)
Average:		2.11	- 0(3')	2.01(2)	- 0(4)	1.52(2)
			- 0(4)	2.37(2)	Average:	1.54
			- 0(4')	2.10(2)		
			Average:	2.15		

The estimated standard deviations are given in parentheses.

of the spectrometer used. Thus iron in the two positions must have very similar hyperfine parameters, with a difference in peak positions less than 0.05 mm/s. A detailed study of Fe-sarcopside showed a low velocity peak with $W = 0.27$ mm/s and an intensity of 49.7%; the high-velocity peak had $W = 0.29$ mm/s and intensity 50.3%. M1 and M2 are both occupied by iron in $\text{Fe}_3(\text{PO}_4)_2$, so the separation of the two high-velocity peaks is ~ 0.02 mm/s larger than that of the two low-velocity peaks. The almost equal intensities of the profiles also show that there are no texture effects (Ericsson and Wäpling, 1976, cf. also Fig. 3).

In hydrothermally prepared $(\text{Ni}_{1-x}\text{Fe}_x)_3(\text{PO}_4)_2$ -sarcopsides with $x \geq 2/3$ some iron must necessarily occupy the M1 sites. As the half-widths obtained in the fittings with only one doublet are approximately constant, ~ 0.28 mm/s, the slight decrease observed in ΔE_Q with x is most easily understood as a result of increased distortions in the MO_6 octahedra (Ingalls, 1964).

Mattievich and Danon (1977) have also studied ferrous phosphates using Mössbauer spectroscopy. For a synthetic Fe-sarcopside they obtained $\text{CS}/\Delta E_Q = 1.19/2.92$ mm/s at room temperature, in reasonable agreement with our values (Table 4). Moreover, Annersten and Nord (1980) reported $\text{CS}/\Delta E_Q = 1.19/3.01$ mm/s at room temperature for $(\text{Mg}_{0.80}\text{Fe}_{0.20})_3(\text{PO}_4)_2$ -sarcopside, prepared at 30 kbar and 873 K. Thus the replacement of nickel by

Table 4. Mössbauer parameters of $(\text{Ni}_{1-x}\text{Fe}_x)_3(\text{PO}_4)_2$ at room temperature

Sample	CS (mm/sec) ^a	ΔE_Q (mm/sec) ^b	W (mm/sec) ^c
$\text{Ni}_{0.9}\text{Fe}_{0.1}\cdots$	1.20	3.09	0.24
$\text{Ni}_{0.8}\text{Fe}_{0.2}\cdots$	1.20	3.04	0.26
$\text{Ni}_{0.7}\text{Fe}_{0.3}\cdots$	1.21	3.06	0.26
$\text{Ni}_{0.6}\text{Fe}_{0.4}\cdots$	1.20	3.07	0.27
$\text{Ni}_{0.5}\text{Fe}_{0.5}\cdots$	1.21	3.00	0.28
$\text{Ni}_{0.4}\text{Fe}_{0.6}\cdots$	1.20	3.07	0.28
$\text{Ni}_{0.3}\text{Fe}_{0.7}\cdots$	1.21	2.99	0.27
$\text{Ni}_{0.15}\text{Fe}_{0.85}\cdots$	1.22	2.96	0.28
$\text{Fe}_3(\text{PO}_4)_2$	1.21	2.93	0.28

a) CS = Centroid Shift relative to an iron foil at room temperature.

b) ΔE_Q = quadrupole splitting, i.e. the peak separation in a doublet.

c) W = full width at half maximum.

The precision in the fitting procedure is ± 0.01 mm/sec in CS and W, ± 0.02 mm/sec in ΔE_Q .

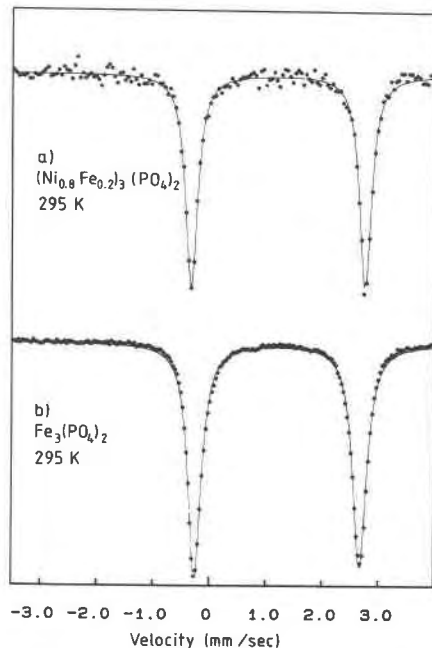


Fig. 3. Room temperature Mössbauer spectra of (a) $(\text{Ni}_{0.8}\text{Fe}_{0.2})_3(\text{PO}_4)_2$ and (b) $\text{Fe}_3(\text{PO}_4)_2$ -sarcopside.

magnesium does not significantly affect the hyperfine parameters.

Mössbauer measurements at elevated temperatures

The close overlap of the two Mössbauer doublets at room temperature rendered an accurate cation distribution determination impossible for the (Ni,Fe)-sarcopsides. The situation is similar in fayalite (Kündig et al., 1967) and (Mg,Fe)-olivine. However, the two doublets in these olivines are partly resolved at temperatures above 500 K (Virgo and Hafner, 1972). The same is also true for (Ni,Fe)-olivines (Annersten et al., 1982). We therefore selected $\text{Fe}_3(\text{PO}_4)_2$ and $(\text{Ni}_{0.50}\text{Fe}_{0.50})_3(\text{PO}_4)_2$ for further Mössbauer studies at elevated temperatures (Table 5 and Fig. 4).

Only one doublet could be resolved between 295 K and 853 K in $(\text{Ni}_{0.50}\text{Fe}_{0.50})_3(\text{PO}_4)_2$. However, in $\text{Fe}_3(\text{PO}_4)_2$ -sarcopside the asymmetry of the low- and high-velocity profiles is obvious above 475 K, indicating two doublets. The intensities of the M1 and M2 doublets were constrained to be 1:2 because there are twice as many M2 as M1 sites. A model with $\Delta E_Q(\text{M2}) > \Delta E_Q(\text{M1})$ gave a somewhat lower least-squares sum than the opposite assignment. In the (Ni,Fe)-olivines studied by Annersten et al. (1982) using Mössbauer spectroscopy around 670 K, $\text{CS}/\Delta E_Q$ was $\sim 0.8/1.8$ mm/s for M1 and $\sim 0.9/2.2$ for M2, i.e., again $\Delta E_Q(\text{M2}) > \Delta E_Q(\text{M1})$. The single doublet obtained for $(\text{Ni}_{0.50}\text{Fe}_{0.50})_3(\text{PO}_4)_2$ at all temperatures is attributed to iron in the M2 sites, in accordance with the postulated strong cation ordering. The somewhat larger

Table 5. Mössbauer parameters obtained at elevated temperatures for $\text{Fe}_3(\text{PO}_4)_2$ - and $(\text{Ni}_{0.50}\text{Fe}_{0.50})_3(\text{PO}_4)_2$ -sarcopsides

Temp (K)	Sites (M1,M2)	CS (mm/sec)	ΔE_Q (mm/sec)	W (mm/sec)
$\text{Fe}_3(\text{PO}_4)_2$:				
475	M1*	1.03	2.67	0.25
	M2*	1.10	2.75	0.25**
573	M1	0.96	2.47	0.26
	M2	1.02	2.59	0.26
618	M1	0.92	2.39	0.25
	M2	0.98	2.51	0.25
$(\text{Ni}_{0.5}\text{Fe}_{0.5})_3(\text{PO}_4)_2$:				
408	M2	1.13	2.90	0.28
540	M2	1.03	2.68	0.28
614	M2	0.97	2.54	0.28
724	M2	0.90	2.34	0.28
770	M2	0.86	2.24	0.27
820	M2	0.82	2.14	0.27
853	M2	0.80	2.05	0.28

For definition of parameters and precisions, see footnote to Table 4.

* The intensities of the M1- and M2-doublets were fixed to 1:2.

** The half widths of the M1- and M2-doublets were constrained (underlined value) to be equal.

$\Delta E_Q(\text{M2})$ value compared to pure $\text{Fe}_3(\text{PO}_4)_2$ is due to an increased nickel content. This effect is much less pronounced in the (Ni,Fe)-olivines (Annersten et al., 1982), indicating a larger octahedral distortion in the (Ni,Fe)-sarcopsides. Incorporation of magnesium in fayalite, on the other hand, also results in an increase of ΔE_Q at elevated temperatures (Bush et al., 1970).

The centroid shift in $(\text{Ni}_{0.50}\text{Fe}_{0.50})_3(\text{PO}_4)_2$ decreases by $7.3 \cdot 10^{-4} \text{ mm} \cdot \text{s}^{-1} \cdot \text{K}^{-1}$, which agrees with the high temperature limit of the second order Doppler shift

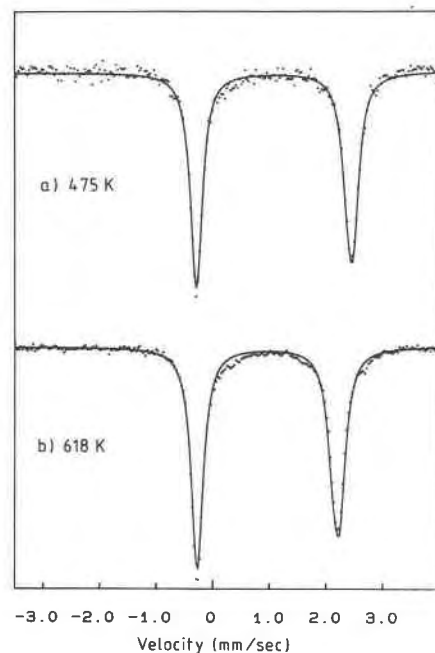


Fig. 4. Mössbauer spectra of $\text{Fe}_3(\text{PO}_4)_2$ -sarcopside at (a) 475 K, (b) 618 K.

(Cohen, 1976, p. 27). Thus the thermal expansion of the crystal does not seem to significantly affect the M2 isomer shifts. This is also observed for M1 in $\text{Fe}_3(\text{PO}_4)_2$ (Fig. 5). At room temperature, a weighted average for the centroid shifts of iron can be estimated from

$$\text{CS(average)} = (\text{CS(M1)} + 2 \cdot \text{CS(M2)})/3$$

This approximation is used in Figure 5 and (analogously) for ΔE_Q in Figure 6. According to Figures 5 and 6, the main reason for the increased resolution with temperature is different variations for $\Delta E_Q(\text{M1})$ and $\Delta E_Q(\text{M2})$. Optimum resolution is obtained around 600 K, but it is still not good enough for an accurate determination of the $\text{Ni}^{2+}/\text{Fe}^{2+}$ ordering.

Mössbauer measurements at low temperatures

The iron-rich sarcopsides $(\text{Ni}_{0.30}\text{Fe}_{0.70})_3(\text{PO}_4)_2$, $(\text{Ni}_{0.15}\text{Fe}_{0.85})_3(\text{PO}_4)_2$ and $\text{Fe}_3(\text{PO}_4)_2$ were studied at temperatures down to 10 K, at which temperature they are magnetically ordered with saturated hyperfine fields B_{hf} (Table 6, Fig. 7). The magnetic transition temperature for $\text{Fe}_3(\text{PO}_4)_2$ -sarcopside is 44 K. Iron clearly occupies one magnetically ordered and one non-magnetic site. As the magnetic interaction ($B_{\text{hf}} \approx 13.8$ Tesla) is not considerably stronger than the electric interaction ($\Delta E_Q \approx 3.07$ mm/s), the full Hamiltonian has been used in the fitting procedure with theoretical peak intensities, using a least-squares fitting program under development at the Institute of Physics, University of Uppsala. The quadrupole splitting ΔE_Q , defined as in the non-magnetic case ($1/2 \cdot eQV_{zz}\sqrt{1 + \eta^2/3}$) has been calculated as described by Karyagin (1966) and later by van Dongen et al. (1975).

The intensities obtained in the fitting of the $\text{Fe}_3(\text{PO}_4)_2$

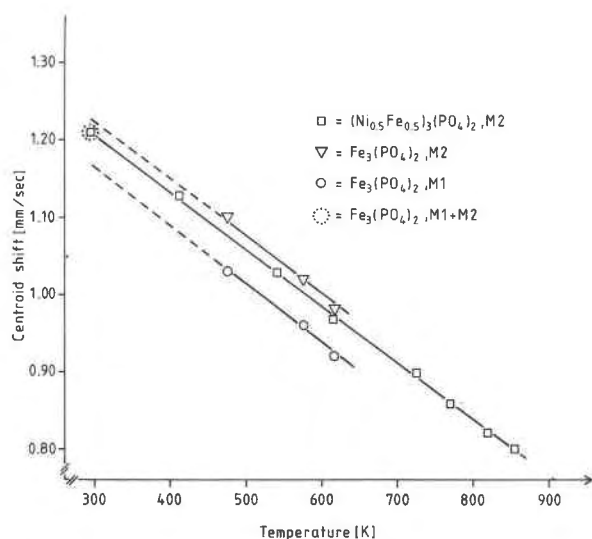


Fig. 5. The centroid shift for iron at M1 and M2 as a function of temperature for $\text{Fe}_3(\text{PO}_4)_2$ -sarcopside and $(\text{Ni}_{0.50}\text{Fe}_{0.50})_3(\text{PO}_4)_2$. For the former phase only an average centroid shift was measured at room temperature (the dotted circle).

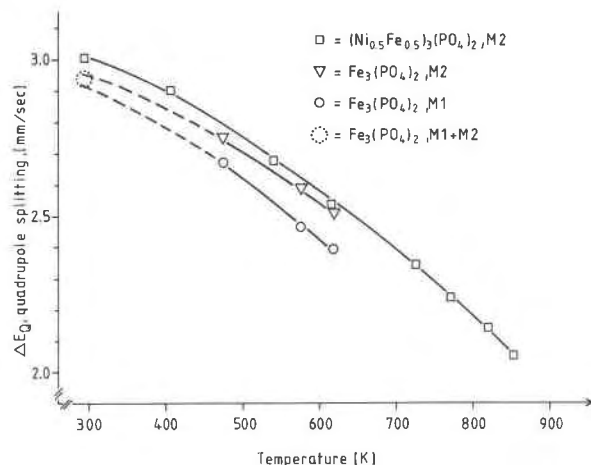


Fig. 6. The quadrupole splitting ΔE_Q for iron at M1 and M2 in $\text{Fe}_3(\text{PO}_4)_2$ and $(\text{Ni}_{0.50}\text{Fe}_{0.50})_3(\text{PO}_4)_2$ versus temperature. For the former phase only an average value was measured at room temperature (the dotted circle).

12.4 K spectrum unambiguously assign the crystallographic sites. The twofold M1 site (33% relative intensity) gives the non-magnetic pattern, the four-fold M2 site (67% intensity) gives the magnetic pattern. The intensities also show that the two sites have almost equal Debye temperatures and also that thickness effects do not significantly affect the intensities.

A comparison of the spectra in Figure 7 clearly shows that nickel preferentially occupies the M1 site, in agreement with our working hypothesis. Assuming equal f -factors (recoil-less fractions of the 14.4 keV radiation) for iron at M1 and M2, the fraction of iron at each site is obtained from:

$$X_{\text{Fe}}(\text{M1}) = x \cdot \text{Int}(\text{M1}) \cdot N(\text{M1+M2})/N(\text{M1})$$

$$X_{\text{Fe}}(\text{M2}) = x \cdot \text{Int}(\text{M2}) \cdot N(\text{M1+M2})/N(\text{M2})$$

Here x denotes the concentration of iron in $(\text{Ni}_{1-x}\text{Fe}_x)_3(\text{PO}_4)_2$, $N(\text{M})$ is the site multiplicity number of "M" sites in the crystal, and $\text{Int}(\text{M})$ is the ^{57}Fe intensity of the M-site signal. In $(\text{Ni}_{0.30}\text{Fe}_{0.70})_3(\text{PO}_4)_2$ $X_{\text{Fe}}(\text{M1})$ is 0.17 and $X_{\text{Fe}}(\text{M2})$ around 0.97, thus indicating a very strong preference of iron for M2 (Table 6).

Discussion

Like the olivine structure, sarcopside consists of hexagonally close-packed layers of oxygen atoms. The two distinct MO_6 octahedra are connected by edge- and corner-sharing. $\langle \text{M2-O} \rangle$ is slightly longer than $\langle \text{M1-O} \rangle$; $(\text{M2})\text{O}_6$ also has a slightly larger scatter in metal-oxygen distances and O-M-O angles than $(\text{M1})\text{O}_6$, and it has the lower point symmetry. This is also true for olivine, although both octahedra are more regular than the corresponding octahedra in sarcopside. The point symmetries

Table 6. Mössbauer parameters of $(\text{Ni}_{1-x}\text{Fe}_x)_3(\text{PO}_4)_2$ at low temperatures together with Fe site occupancies

Sample	Temp (K)	M1				M2				
		CS ^a	ΔE_Q^b	Int.	X_{Fe}^d	CS ^a	ΔE_Q^b	B ^c	Int.	X_{Fe}^d
$\text{Fe}_3(\text{PO}_4)_2$	12.4	1.32	3.02	0.33	0.99	1.38	3.07	13.7	0.67	1.01
$\text{Ni}_{0.15}\text{Fe}_{0.85}$	10	1.32	3.13	0.18	0.47	1.36	3.04	13.7	0.82	1.04
$\text{Ni}_{0.3}\text{Fe}_{0.7}$	10	1.26	3.23	0.08	0.17	1.37	3.10	13.9	0.92	0.97

a) The centroid shift is in mm/sec and relative to α -Fe at room temperature.

b) The quadrupole splitting is in mm/sec and defined as $\frac{1}{2}eQV_{ZZ}\sqrt{1+\eta^2/3}$, where the parameters have their conventional meanings.

c) The (saturated) hyperfine field is given in tesla.

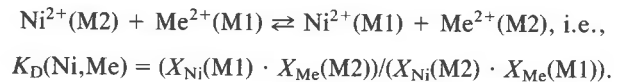
d) X_{Fe} is the fraction of the M site occupied by Fe.

The precisions in the fitting procedure are: CS = ± 0.01 , ΔE_Q and Int. = ± 0.02 , B = ± 0.1

for M1 and M2 are \bar{l} and l in sarcopside, and \bar{l} and m in olivine.

The strong cation ordering in the (Ni,Fe)-sarcopsides will be quantified by means of a cation distribution coefficient, K_D . Assuming equal activity factors of the cations, $K_D(\text{Ni,Me})$ for a $(\text{Ni}_{1-x}\text{Me}_x)_3(\text{PO}_4)_2$ -sarcopside might be regarded as the equilibrium constant for the

cation exchange reaction



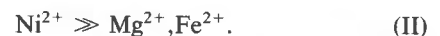
Our low-temperature Mössbauer data (Table 6) show that $K_D(\text{Ni,Fe})$ is very large, ~ 100 , for the samples synthesized at 1 bar, 1070 K. The Gibbs' free energy change $\Delta G^\circ = -RT \ln K_D$ is about $-40 \text{ kJ} \cdot \text{mole}^{-1}$ at 1070 K.

The fact that the graffonite structure (6,5,5-coordinated cations) is the stable phase for $\text{Fe}_3(\text{PO}_4)_2$ at 1 bar, while $\text{Fe}_3(\text{PO}_4)_2$ -sarcopside (6,6-coordinated cations) should rather be regarded as a high-pressure phase, agrees with earlier observations that Fe^{2+} has a rather strong preference for five-coordination sites (Nord and Ericsson, 1982b). Ni^{2+} with its great tendency for six-coordination (Burns, 1970) obviously acts as a stabilizer for the (Ni,Fe)-sarcopsides.

Some other cation distribution studies of (Ni,Me) $_3(\text{PO}_4)_2$ -sarcopsides have recently been completed. These results show that $K_D(\text{Ni,Zn}) = 4$ (Nord, 1982) and $K_D(\text{Ni,Mg}) = 4.0$ (Nord and Stefanidis, 1983). Accordingly, Ni^{2+} consistently orders at the slightly smaller and somewhat more regular M1 sites, in agreement with predictions of Burns (1970). The ionic preference order for M1 over M2 in sarcopside may be given as



Recent studies of synthetic (Ni,Fe)-olivines have shown a rather strong cation ordering with $K_D(\text{Ni,Fe}) \approx 10$ for phases annealed at 1270 K, so again Ni^{2+} strongly prefers the M1 sites (Annersten et al., 1982). The cation distribution has also been determined in some (Ni,Mg)-olivines. Bish (1981) obtained $K_D(\text{Ni,Mg}) = 9.9 \pm 0.4$ at 770 K, while Rajamani et al. (1975) reported $K_D(\text{Ni,Mg}) = 9.2$ at about 1500 K. Judging from these K_D values, the cation preference order for M1 in olivine is



This observation agrees well with earlier observations that the $\text{Mg}^{2+}/\text{Fe}^{2+}$ distribution in olivine is almost ran-

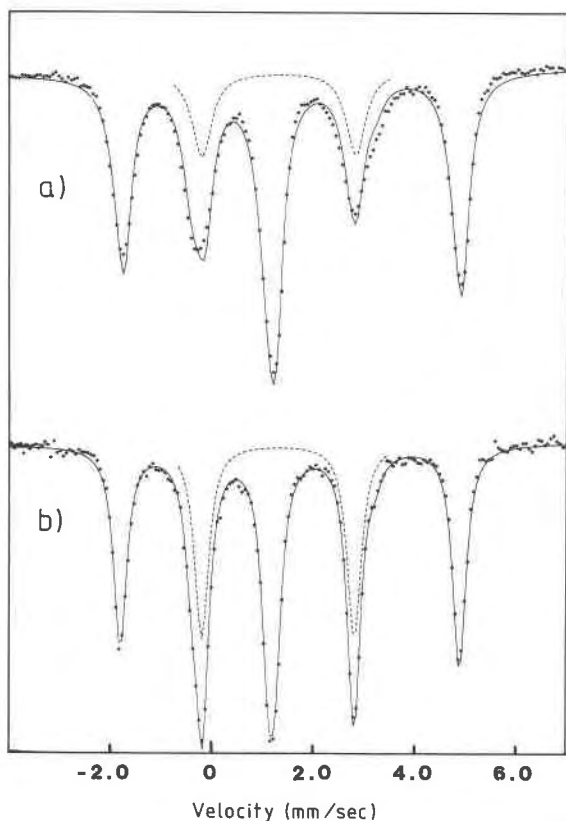


Fig. 7. Low-temperature Mössbauer spectra: (a) $(\text{Ni}_{0.15}\text{Fe}_{0.85})_3(\text{PO}_4)_2$ at 10 K, (b) $\text{Fe}_3(\text{PO}_4)_2$ -sarcopside at 12.4 K. The dashed doublet in each spectrum is attributed to iron at the non-magnetic M1 site.

dom (e.g., Brown, 1980), and with results for two (Mg,Fe,Ni)₂SiO₄-olivines (Nord et al., 1982).

In Ni₂SiO₄, (M2-O) is somewhat longer than (M1-O); the difference between the two averaged M-O distance values is 0.022 Å (Lager and Meagher, 1978). In Ni₃(PO₄)₂ this difference is only 0.003 Å (Calvo and Faggiani, 1975). Yet the Ni²⁺/Fe²⁺ ordering is *stronger* in sarcopside than in olivine, although Fe²⁺ is significantly larger than Ni²⁺, so we conclude that the size effects are slight in these phases. As regards the Ni²⁺/Mg²⁺ partitioning, the situation is reversed; the ordering is now stronger in olivine. Mg²⁺ is only slightly (~0.03 Å in radius) larger than Ni²⁺ (Shannon, 1976). We therefore conclude that crystal field stabilization energies rather than size effects are responsible for the observed Ni-Mg-Fe cation ordering in olivine and sarcopside. Additional Ni²⁺/Me²⁺ cation distribution studies, based on crystal structures with octahedra similar in shape and symmetry to those in sarcopside and olivine, are in progress to help clarify these interesting matters on cation ordering.

Acknowledgments

We are grateful to Mr. Per Jernberg and Mr. Tore Sundqvist (Institute of Physics, Uppsala), who allowed us to use their Mössbauer fitting program, capable of handling the full Hamiltonian, prior to publication. We are indebted to Professor Hans Annersten (University of Uppsala) and Dr. Bengt Lindqvist (Swedish Museum of Natural History) for their critical reading of the manuscript.

We also want to thank Miss Kersti Gløersen (Uppsala) for her skillful typing and linguistic correction of the manuscript, and Mr. Sten Åhlin (Studsvik) for his willing help during the collection of the neutron diffraction data.

The generous financial support from the Swedish Natural Science Research Council (NFR) is gratefully acknowledged.

References

- Annersten, H., Ericsson, T., and Filippidis, A. (1982) Cation ordering in Ni-Fe olivines. *American Mineralogist*, 67, 1212-1217.
- Annersten, H., Ericsson, T., and Nord, A. G. (1980) The cation ordering in iron-containing zinc and magnesium orthophosphates determined from Mössbauer spectroscopy. *Journal of the Physics and Chemistry of Solids*, 41, 1235-1240.
- Annersten, H. and Nord, A. G. (1980) A high pressure phase of magnesium orthophosphate. *Acta Chemica Scandinavica*, A34, 389-390.
- Bish, D. L. (1981) Cation ordering in synthetic and natural Ni-Mg olivines. *American Mineralogist*, 66, 770-776.
- Brown, G. E. (1980) Olivines and silicate spinels. In P. H. Ribbe, Ed., *Orthosilicates*, vol. 5, p. 275-281. Reviews in Mineralogy. Mineralogical Society of American, Washington, D.C.
- Burns, R. G. (1970) *Mineralogical Applications of Crystal Field Theory*. Cambridge University Press, Cambridge.
- Bush, W. R., Hafner, S. S., and Virgo, D. (1970) Some ordering of iron and magnesium at the octahedrally coordinated sites in a magnesium-rich olivine. *Nature*, 227, 1339-1341.
- Calvo, C. and Faggiani, R. (1975) Structure of nickel orthophosphate. *Canadian Journal of Chemistry*, 53, 1516-1520.
- Cohen, R. L. (1976) *Applications of Mössbauer Spectroscopy*, Vol. I. Academic Press, New York, San Francisco, London.
- van Dongen Torman, J., Jagannathan, R., and Trooster, J. M. (1975) Analysis of ⁵⁷Fe Mössbauer hyperfine spectra. *Hyperfine Interactions*, 1, 135-144.
- Ericsson, T. and Wäppling, R. (1976) Texture effects in 3/2-1/2 Mössbauer spectra. *Journal de Physique*, 37, Colloque C6, 719-723.
- Ingalls, R. (1964) Electric-field gradient tensor in ferrous compounds. *Physical Review*, 133A, 787-795.
- Karyagin, S. V. (1966) Determination of the local field parameters in Mössbauer hyperfine spectra. *Soviet Physics Solid State*, 8, 391-396.
- Kostiner, E. and Rea, J. R. (1974) Crystal structure of ferrous phosphate, Fe₃(PO₄)₂. *Inorganic Chemistry*, 13, 2876-2880.
- Kündig, W., Cape, J. A., Lindqvist, R. H., and Constabaris, G. (1967) Some magnetic properties of Fe₂SiO₄ from 4 K to 300 K. *Journal of Applied Physics*, 38, 974-948.
- Lager, G. A. and Meagher, E. P. (1978) High-temperature structural study of six olivines. *American Mineralogist*, 63, 365-377.
- Mattievich, E. and Danon, J. (1977) Hydrothermal synthesis and Mössbauer studies of ferrous phosphates of the homologous series Fe₃(PO₄)₂(H₂O)_n. *Journal of Inorganic and Nuclear Chemistry*, 39, 569-580.
- Moore, P. B. (1972) Sarcopside: its atomic arrangement. *American Mineralogist*, 57, 24-35.
- Nord, A. G. (1982) A neutron diffraction study of the olivine-related solid solution (Ni_{0.75}Zn_{0.25})₃(PO₄)₂. *Neues Jahrbuch für Mineralogie*, 422-432.
- Nord, A. G., Annersten, H., and Filippidis, A. (1982) The cation distribution in synthetic Mg-Fe-Ni olivines. *American Mineralogist*, 67, 1206-1211.
- Nord, A. G. and Ericsson, T. (1982a) The cation distribution in synthetic (Fe,Mn)₃(PO₄)₂ graffonite-type solid solutions. *American Mineralogist*, 67, 826-832.
- Nord, A. G. and Ericsson, T. (1982b) Cation distribution in (Fe_{1-x}Me_x)₃(PO₄)₂ graffonite-type solid solutions determined by Mössbauer spectroscopy. *Zeitschrift für Kristallographie*, 161, 209-224.
- Nord, A. G. and Kierkegaard, P. (1980) Crystal chemistry of some anhydrous divalent-metal phosphates. *Chemica Scripta*, 15, 27-39.
- Nord, A. G. and Stefanidis, T. (1983) Crystallographic studies of some olivine-related (Ni,Mg)₃(PO₄)₂ solid solutions. *Physics and Chemistry of Minerals*, 10, 10-15.
- Rajamani, V., Brown, G. E., and Prewitt, C. T. (1975) Cation ordering in Ni-Mg olivine. *American Mineralogist*, 60, 292-299.
- Rietveld, H. M. (1969) A profile refinement method for nuclear and magnetic structures. *Journal of Applied Crystallography*, 2, 65-71.
- Scott, H. G. (1983) The estimation of standard deviations in powder diffraction Rietveld refinements. *Journal of Applied Crystallography*, 16, 159-163.
- Shannon, R. D. (1976) Revised effective ionic radii and systematic studies of interatomic distances in halides and chalcogenides. *Acta Crystallographica*, A32, 751-767.
- Virgo, D. and Hafner, S. S. (1972) Temperature-dependent Mg,Fe distribution in a lunar olivine. *Earth and Planetary Science Letters*, 14, 305-312.